



OPEN Photodynamic inactivation and its effects on the heterogeneity of bacterial resistance

Jennifer M. Soares^{1✉}, Vladislav V. Yakovlev², Kate C. Blanco¹ & Vanderlei S. Bagnato^{1,2}

Antimicrobial resistance is a growing threat to global public health, requiring innovative approaches for its control. Photodynamic inactivation (PDI) with light-activated photosensitizers has emerged as a strategy to combat resistant bacteria, challenging the intrinsic heterogeneity of bacterial populations. This study evaluates the impact of PDI on both heterogeneity and shape of the distribution profile of resistant bacterial populations, specifically on strains of *Staphylococcus aureus* resistant to amoxicillin, erythromycin, and gentamicin, for exploring its potential as an adjuvant therapy in the fight against bacterial resistance. Curcumin (10 μM) was used as a photosensitizer and five cycles of PDI were applied on *Staphylococcus aureus* strains under 450 nm irradiation of 10 J/cm² energy density. The resistance variations amongst bacterial subpopulations were investigated by calculating the minimum inhibitory concentration (MIC) before and after PDI treatment. MIC was significantly reduced by the antibiotics tested post-PDI and a reduction in the heterogeneity of bacterial populations was recorded, suggesting PDI can effectively decrease the resistance diversity of *Staphylococcus aureus*. The result reinforces the potential of PDI as a valuable adjuvant therapy, offering a promising avenue for mitigating bacterial resistance and promoting more effective treatment strategies against resistant infections.

The heterogeneity of a population of microorganisms under infection treatment is a critical aspect that influences both the dynamics of infection and the effectiveness of treatment¹. During such treatments, microbial populations are subject to a variety of selective pressures, including exposure to antimicrobials², which select resistant microorganisms and can induce variations in their survival capacity, growth, and virulence, contributing to a complex heterogeneity³. Historically, the main causes of human mortality were associated with infectious diseases^{4,5}, since they are easily contagious and treatments were ineffective until the discovery of Penicillin, the first antibiotic⁶, in 1928. Because of that drug, life expectancy has increased and, currently, the main fatal diseases are associated with cardiovascular problems and cancer^{4,7,8}. However, the rise of antibiotic-resistant pathogens has increased alarmingly, and future projections indicate infectious diseases will be the main causes of human mortality, reaching up to 10 million annually^{7,9}, returning to a similar scenario of the past¹⁰.

The presence of resistant subpopulations and the rapid adaptation capacity of microorganisms can lead to therapeutic failure, requiring the use of drug combinations or the development of new antimicrobials³. Treatments of infections can not only select local resistant microorganisms but also facilitate the transfer of resistance genes between microorganisms, magnifying the problem of antimicrobial resistance^{11,12}. Microbial heterogeneity can result in significant variations in the responses to treatments between different individuals or infections, making infection management a clinical challenge^{13,14}. A therapy combined with the use of multiple antimicrobials with different mechanisms of action is a strategy to overcome heterogeneity, reduce the risk of selection of resistant subpopulations, and address microbial heterogeneity more effectively¹⁵.

Photodynamic inactivation has been shown useful for enhancing the action of the antibiotic, increasing the susceptibility of bacteria to different classes, and, thus, preventing the spread of resistance^{16–22}. Its mechanism of action is initiated by the uptake of the photosensitizer (PS) by the microorganism, which when it receives a photon with enough energy to promote an electron from the ground state (S_0) to the excited singlet state (S_1). The mechanism of interest is the transition of the electron without radiation to the excited triplet state (T_1) via intersystem crossing, which can return to the ground state by a phosphorescence process^{23–25}. PS in the triplet state can trigger two types of reactions in the microorganism. One refers to the interaction with biomolecules through electron transfer^{26,27}, which, in turn, interacts with oxygen, triggering the production of various reactive oxygen species (ROS) that degrade cellular components and can lead to the death of the microorganism²⁸. Triplet PS, the second mechanism, transfers energy directly to oxygen so that it passes into the singlet state, which is highly reactive for degrading cellular components and can lead to the death of the microorganism^{27,29}.

¹Institute of Physics of São Carlos, University of São Paulo, São Carlos, SP, Brazil. ²Biomedical Engineering, Texas A&M University, College Station, TX, USA. ✉email: jennifermsoares7@gmail.com

This study investigated the photodynamic action on the heterogeneity of resistant bacterial populations, i.e., the different responses of bacterial cells within the population phenotypically classified as resistant, exploring the feasibility of mitigating the emergence of antimicrobial resistance and enhancing therapeutic efficacy. A detailed analysis based on the microbial kill profile is proposed, validating the effectiveness of the approach in combating resistance. Such validation was conducted by quantifying minimum inhibitory concentrations (MIC) for different antibiotics classes and examining the heterogeneous responses of resistant bacterial populations (Fig. 1). A mathematical analysis of the data involved the exploration of functions that adequately describe the behavior of population mortality. The study stands out in its analytical focus on the diversity of responses to PDI, providing valuable information for developing more effective strategies for managing resistant bacterial infections.

Results

Effect of antibiotics on resistant strains without PDI

The data in Fig. 2 show a direct relationship between the concentrations of amoxicillin (AMO), erythromycin (ERY), and gentamicin (GEN) antibiotics and the lethal fraction of resistant bacterial strains for both clinical isolates of methicillin-resistant *Staphylococcus aureus* (MRSA) and laboratory-induced resistance. Notably, resistant strains maintained viability at concentrations substantially higher than the reference minimum inhibitory concentration (MIC), surviving even at doses up to 8 times higher, with only a fraction of the population affected. The logistic function described by Eq. 2 was the one that best modeled the experimental data.

The bacterial death profile of MRSA (Fig. 2.A) was different for the three aforementioned antibiotics, leading to different death fraction derivative curves. Unlike AMO-induced *S. aureus* strains (Fig. 2.B) and ERY-induced *S. aureus* strains (Fig. 2.C), the death fraction profile and the respective derivatives of AMO, ERY, and GEN were similar. The death fraction profile and the derivative of GEN-induced *S. aureus* (Fig. 2.D) were distinct for AMO when compared to ERY and GEN.

The results underscore the complexity of bacterial resistance and the need for assessment methods that adequately capture the heterogeneity of bacterial responses to antimicrobials. The use of logistic functions to model experimental data, such as Eq. 2, has proven particularly effective for the understanding of the behavior of resistant bacterial populations. The differentiation in mortality profiles and derived curves among different strains and antibiotics emphasizes the importance of personalized approaches for the development of antimicrobial therapies toward overcoming the challenges posed by bacterial resistance.

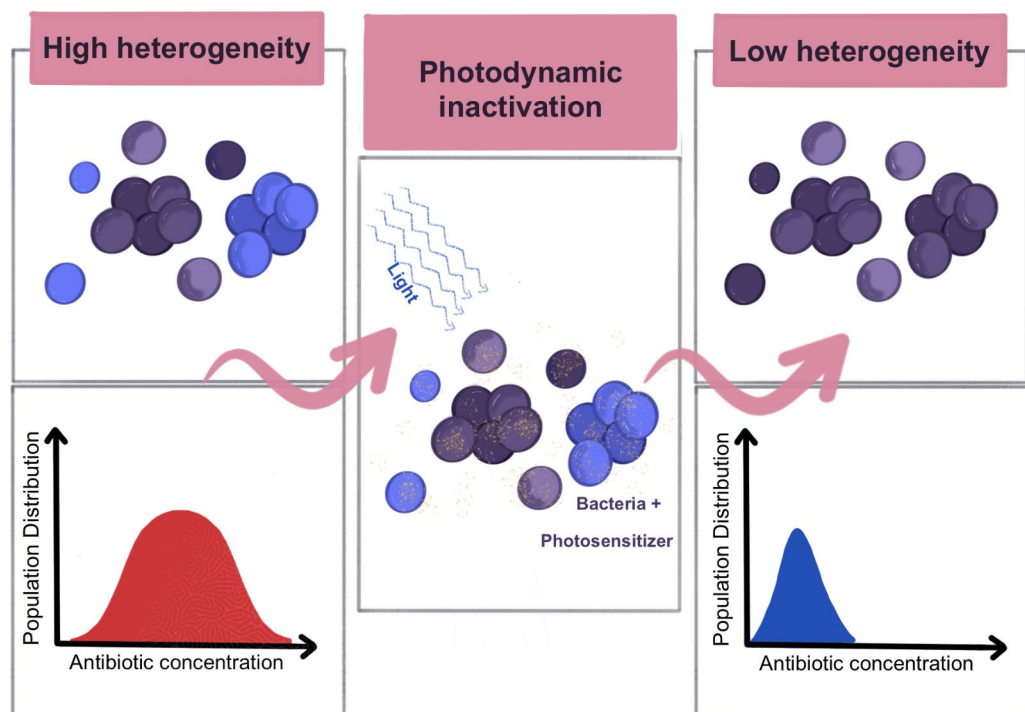


Fig. 1. Bacterial populations with a highly heterogeneous response tend to have broad survival fractions at different antibiotic concentrations, usually indicating a resistant phenotype. By using photodynamic inactivation, i.e. irradiating bacterial cultures with a photosensitizer, cells that survive oxidative stress are more homogeneous in their response to antibiotics, similar to phenotypically sensitive profiles.

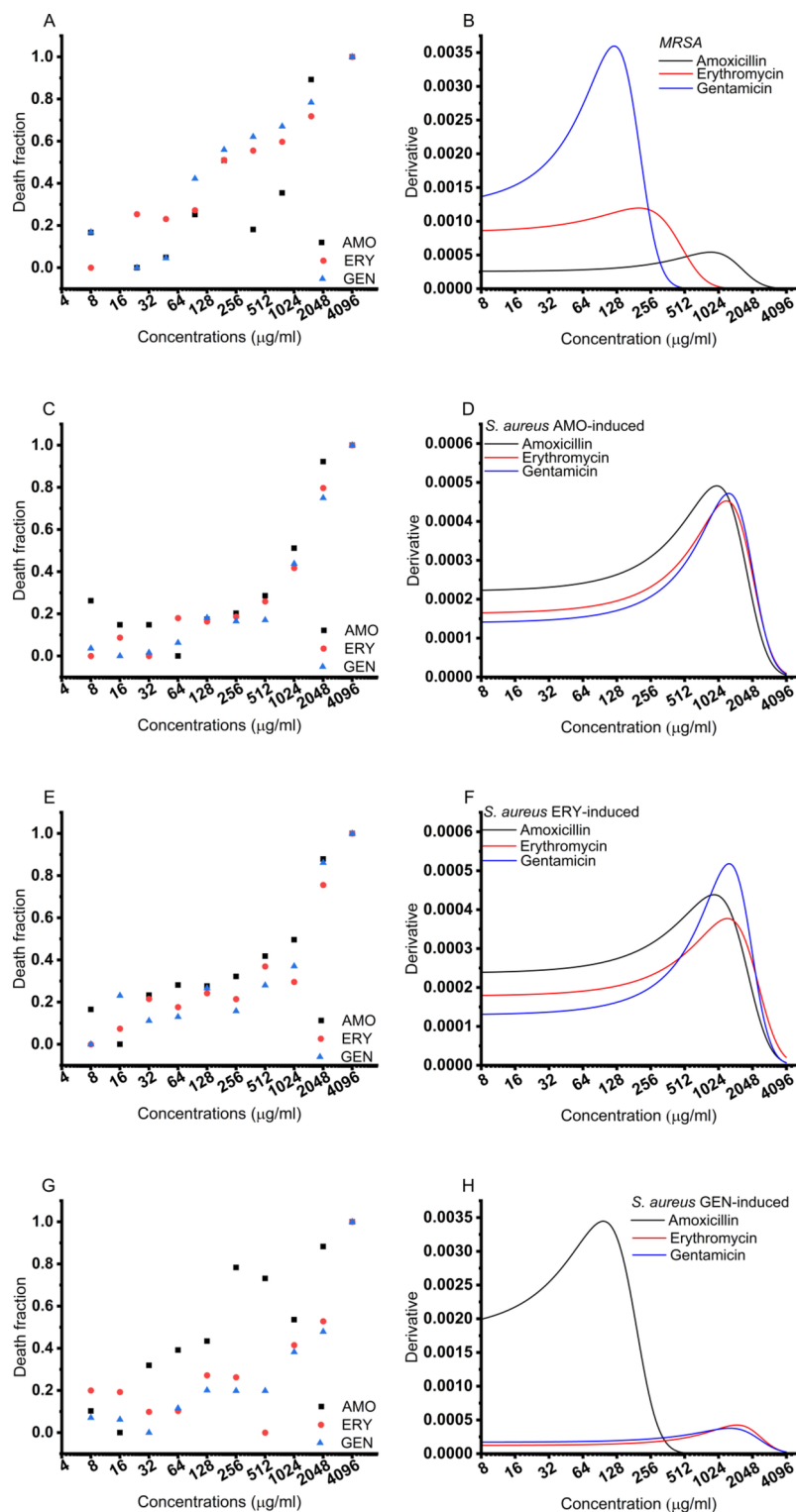


Fig. 2. Population death fraction of resistant strains by different concentrations of amoxicillin (AMO), erythromycin (ERY), and gentamicin (GEN) for bacteria with no prior photodynamic inactivation (PDI) treatment and respective derivative of the death fraction curve of (A) methicillin-resistant *Staphylococcus aureus* (MRSA), (B) *Staphylococcus aureus* resistance induced by AMO, (C) *Staphylococcus aureus* resistance induced by ERY, and (D) *Staphylococcus aureus* resistance induced by GEN.

Effect of antibiotics on resistant strains with PDI

The death profile for the strains that show an increased susceptibility to different antibiotics (see³⁰) after PDI cycles are best modeled by the logistic function provided by Eq. 3 (Fig. 3). When compared to the concentrations displayed in Fig. 2, the mortality fraction is seen at lower concentrations, reaching total death at concentrations that result in up to 87.5% reduction. AMO, ERY, and GEN antibiotics produced identical mortality profiles and derivative curves for MRSA and AMO-induced and ERY-induced *S. aureus* (Fig. 3.A-C). However, GEN-induced *S. aureus* (Fig. 3.D) showed a different killing profile and derivative curves for GEN compared to AMO and ERY.

The application of PDI as a pre-treatment is an effective strategy to increase the susceptibility of antibiotic-resistant bacterial strains, showing potential as a therapeutic adjuvant in the fight against antimicrobial resistance. The PDI conditions applied (10 μ M, 10 J/cm²) resulted in a reduction of the bacteria load to 2–3 log(CFU/ml). It is noteworthy that the initial number of bacteria was standardized at each cycle to maintain consistency. Modeling the kill profile by a logistic function (e.g., Eq. 3) provides a robust method for analyses of the effectiveness of PDI, significantly reducing the concentrations of antibiotics necessary for eradicating bacterial populations previously treated with PDI. The similarity between the killing profiles and the derivative curves for MRSA, AMO-induced, and ERY-induced strains indicates an overall positive response to PDI, regardless of the antibiotic tested. However, the distinction observed for GEN-induced strain suggests the efficacy of PDI may vary in function of strain-specific resistance, highlighting the importance of investigating interactions among different types of bacterial resistance and PDI treatment. The results reinforce the feasibility of PDI as a promising intervention for reducing the burden of antimicrobial resistance, suggesting its implementation can significantly improve antibiotic treatment outcomes in infections caused by resistant strains. Such findings can pave the way for future studies aimed at optimizing PDI protocols, exploring their use in combination with antimicrobial agents, and overcoming the challenges posed by antibiotic resistance. However, the practical application of the strategy requires a detailed understanding of the mechanisms by which PDI affects antimicrobial susceptibility and validation of those effects in clinical models.

Comparison of survival curve widths

As shown in Figs. 2 and 3, the MIC of the strains after PDI cycles was reduced and the mathematical description was different, despite maintaining the sigmoid death profile described by the logistic equation. However, not only changes in MIC have been identified³⁰, but also different widths of the distribution curves obtained through the derivative of the death fraction, which is directly related to the heterogeneity of the population's response to the external stimulus, i.e. the difference in the rate of death by the different antibiotics in each bacterial population. Regarding the strains treated with five cycles of PDI, the width of the distribution showed a 76.52% average percentage reduction for MRSA (see Fig. 4.A), with only a 49.05% reduction in the case of GEN. According to Fig. 4.B, AMO-induced *S. aureus* showed a 97.11% average percentage reduction in distribution width, which was similar concerning the three antibiotics – the same for ERY-induced *S. aureus* (Fig. 4.C) with a 97.27% average percentage reduction. The reduction was 90.27% for GEN-induced *S. aureus* (Fig. 4.D), with GEN being highlighted, thus showing a 99.84% percentage reduction. Figure 4 shows the prior application of PDI reduces the heterogeneity of the population that remains after treatment.

Discussion

Antimicrobial resistance is characterized by the ability of bacteria to survive and reproduce above the reference MIC, generally established by microbiological control and surveillance organizations^{13,31}. A bacterium can resist an antibiotic in different ways (e.g., through increased expression of efflux pumps, synthesis of enzymes that degrade antibiotics, modifications, or increased expression of binding sites)³² and several of such alterations occur due to changes in gene expression through either mutations or acquisition of genes via conjugation or transduction^{10,33}.

Gene expression can be subject to slight fluctuations that differ for each cell due to its modulation by positive and negative feedback systems, leading to distinct subpopulations^{3,34}. Therapeutic failure may occasionally result from phenotypic changes caused by stimuli to which a population is exposed. Such changes can affect metabolism in more active ways (e.g., increased efflux pump activity³⁵ and slower metabolism), enabling a population exposed to concentrations of the antibiotic higher than its MIC to survive. In such situations, the population is referred to as tolerant; if it is limited to a subpopulation, it is referred to as persistent^{11,14}. Those are examples that show the response to antibiotics is not homogeneous within a population, especially where bacteria eradication is hampered by phenotypic differences or levels of gene expression of the subpopulations that form them^{13,36,37}.

the hypothesis that populations with weak responses to antibiotics exhibit greater subpopulation heterogeneity, due to the presence of resistant or persistent cells³⁴, is supported by the results in Figs. 2 and 3. In these figures, the death fraction distribution curve extends along the x-axis and shifts toward higher antibiotic concentrations. MRSA is a clinical isolate, which implies that it originated under external conditions that selected for cells capable of surviving and proliferating in high antibiotic concentrations. This makes MRSA a more homogeneous population compared to antibiotic-induced *S. aureus* developed in the laboratory, where increased MIC was observed for other antimicrobial classes beyond the one used to induce resistance³⁰. In other words, the mechanism associated with antibiotic-induced *S. aureus* resistance may be related to metabolic changes, such as expression of efflux pumps and increase in target sites, since the induced class, for example, might be resistant due to an alteration in the binding site or creation of particular enzymes, has not been identified^{31,34}. That is probably one of the reasons for the greater distribution width of the death fraction for resistant bacteria, especially antibiotic-induced ones.

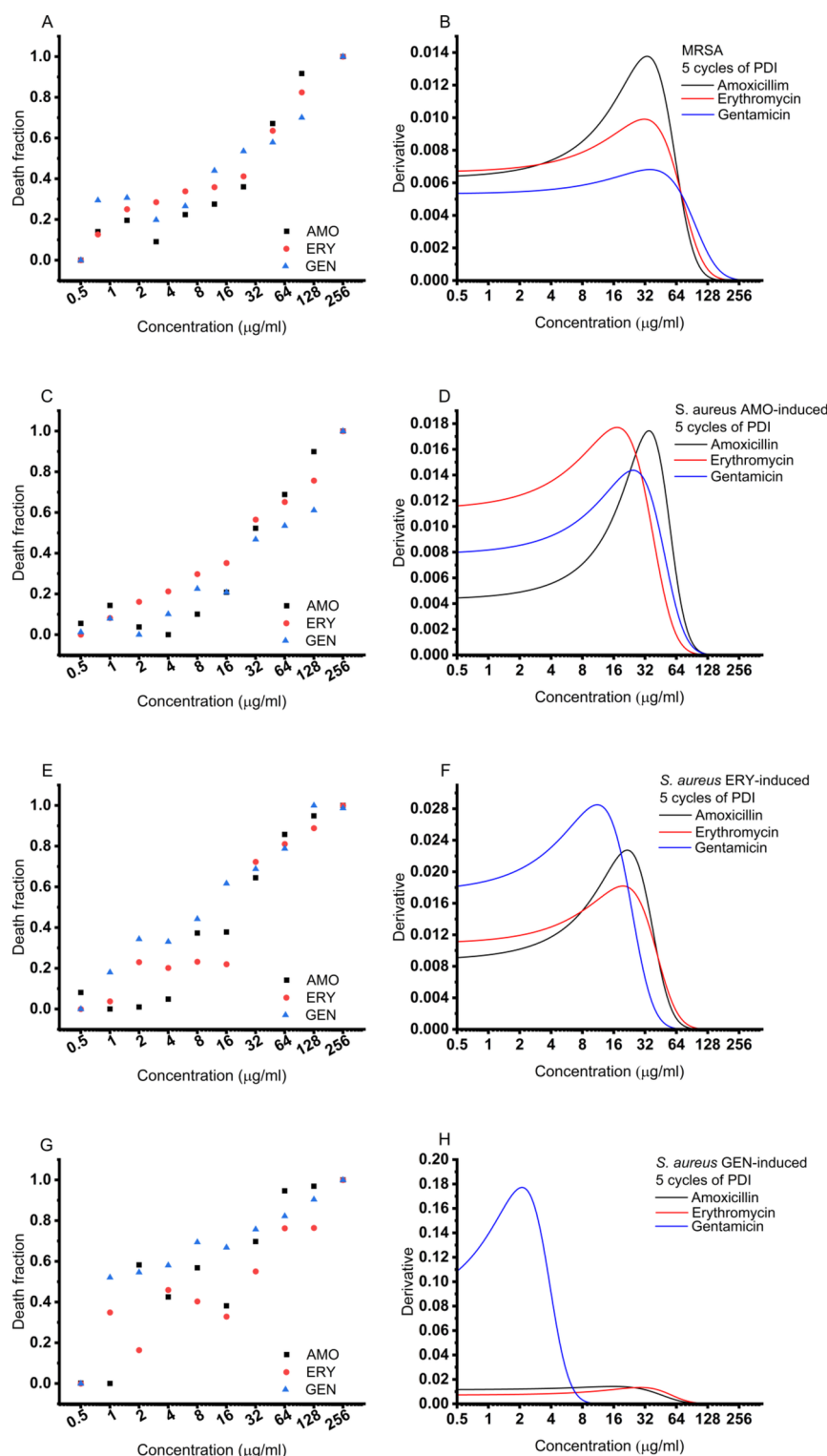


Fig. 3. Population lethal fraction by different concentrations of amoxicillin (AMO), erythromycin (ERY), and gentamicin (GEN) for bacteria treated with five cycles of photodynamic inactivation (PDI) and respective derivative of the death fraction curve of (A) Methicillin-resistant *Staphylococcus aureus* (MRSA), (B) *Staphylococcus aureus* resistance induced by AMO, (C) *Staphylococcus aureus* resistance induced by ERY, and (D) *Staphylococcus aureus* resistance induced by GEN.

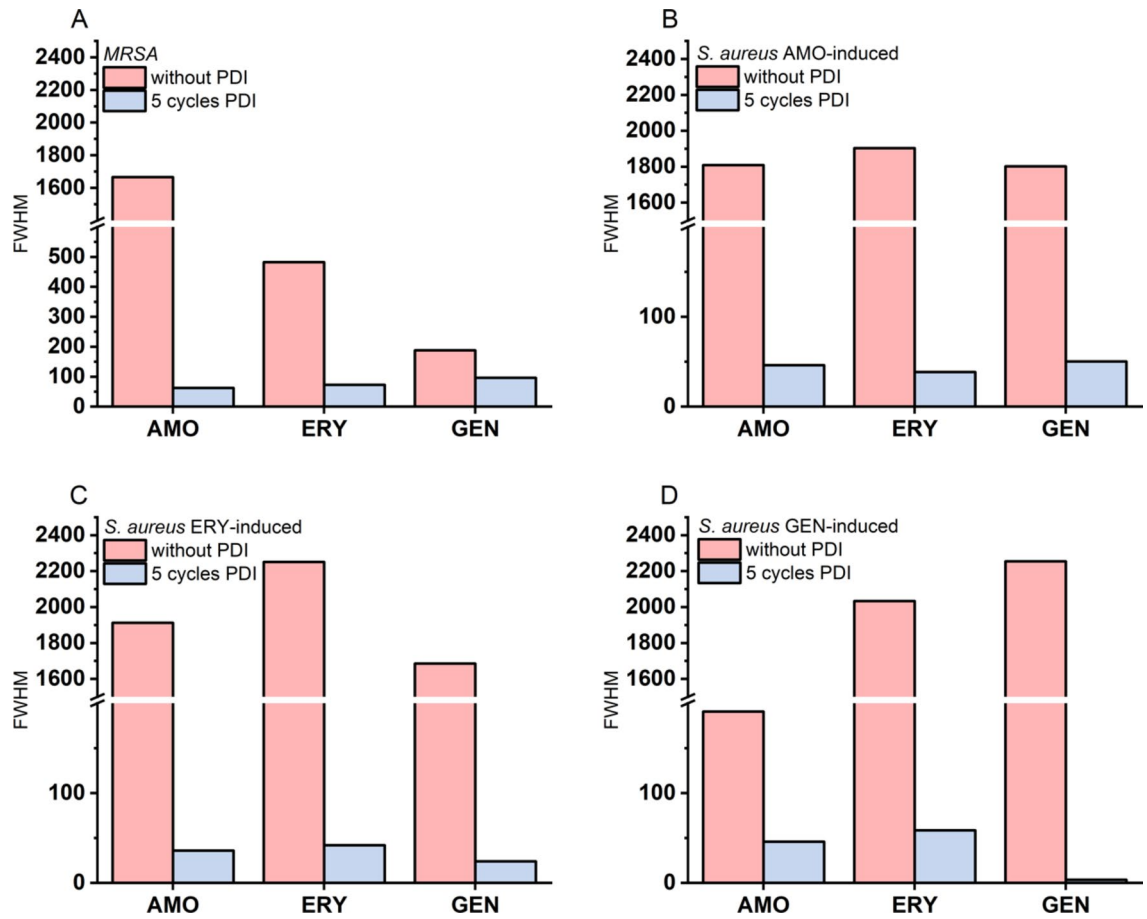


Fig. 4. The full width at half maximum (FWHM) of the distribution curve obtained by the derivative of the survival fraction for amoxicillin (AMO), erythromycin (ERY), and gentamicin (GEN) for strains with no treatment with photodynamic inactivation (PDI) and after 5 cycles of PDI. (A) methicillin-resistant *Staphylococcus aureus* (MRSA), (B) *Staphylococcus aureus* resistance induced by AMO, (C) *Staphylococcus aureus* resistance induced by ERI, and (D) *Staphylococcus aureus* resistance induced by GEN.

Bacteria whose susceptibility to antibiotics increased by photodynamic action showed a shift in the death distribution curve for lower concentrations of the antimicrobials and a narrowing of the width (Figs. 2 and 3). Since those are more susceptible strains, i.e., they respond to the action of the antibiotic, the metabolic variations are expected to be smaller in the function of the more homogeneous response¹⁴. Therefore, the photodynamic effect on a resistant population would eliminate metabolically more active subpopulations over the generations. The literature shows after the application of PDI, the bacterial growth curve is affected by the remaining cells, corroborating that hypothesis³⁸. In other words, the photooxidative action helps to control the different subpopulations and lower the MIC of the antibiotic.

The decision to implement a 6-hour interval for the aPDI cycles was informed by the growth dynamics of *S. aureus* and MRSA, which indicate that bacterial cultures can recover and proliferate effectively within this timeframe. This interval also mirrors clinical practices where antibiotics are commonly administered every 6 to 12 h, allowing us to align our experimental design with relevant therapeutic strategies.

The effectiveness of antibiotic therapy is related to the identification of the bacterial strain's sensitivity profile to the antibiotic³⁹. As a first metric, MIC is the procedure adopted for such verification and can be obtained by different experimental methodologies such as broth microdilution and macrodilution, Etest, and Kirby-Bauer method⁴⁰. The response collected from those experiments is binary, with microbial growth and non-growth concentrations^{34,41}. However, many nuances impact the antibiotic's therapeutic success, requiring information such as subpopulation characteristics to be obtained by another methodology (e.g., population analysis profiling (PAP) assay)⁴².

Resistant populations have fluctuations in the MIC values due to the variability in bacterial cells present in the population^{2,43}. Methodologically, there are limitations to fine-tuning concentrations, as they are tested on a 2-fold scale, with neighboring values being more distant at high concentrations than at low ones. This favors a more precise determination of the MIC experimentally for the most susceptible strains^{44,45}. Given the difference in heterogeneity and MIC determined between the groups without PDI (resistant strains) and the group with five cycles of PDI (strains with increased susceptibility), the results indicate the potential of PDI for reducing

the phenotypic diversity of bacterial populations, leading to a more homogeneous response to antimicrobial treatment and possibly increasing the effectiveness of the antibiotic.

The analysis of the data shown in Figs. 2 and 3, and 4 provided significant information on the impact of PDI on the susceptibility of different strains of *Staphylococcus aureus* to commonly used antibiotics, such as AMO, ERY, and GEN. The mathematical description of cell death - preserving a sigmoid profile, as indicated by the logistic equation - suggests PDI does not significantly change the action of antibiotics on bacteria⁴⁶. However, the variation in the width of the distribution curves, obtained through the derivative of the death fraction, reflects significant changes in the heterogeneity of the population's responses to external stimuli⁴⁷. Specifically, the reduction in distribution width suggests a homogenization of susceptibility within the treated bacterial population, with fewer variations in individual responses to antibiotics. The notable differences in reduced distribution width between strains and antibiotics highlight the complexity of the interaction between PDI and bacterial resistance. A 76.52% average reduction was observed in the distribution width for MRSA strains treated with PDI, whereas the reduction reached 99.84% specifically for GEN for the GEN-induced strain, indicating an almost complete decrease in the heterogeneity of the response to the antibiotic. Such an effect is particularly notable since antibiotic resistance is often mediated by a diversity of genetic and phenotypic mechanisms within the bacterial population^{34,48}.

As demonstrated by the reduction in distribution width, the significant homogenization of bacterial susceptibility after a PDI treatment offers a new perspective on the potential of PDI for mitigating antibiotic resistance. In addition to acting directly on bacteria to induce cell death, PDI can facilitate the action of antibiotics by reducing variability in the bacterial response to the treatment^{24,40,49}. Such an observation is of great importance for the development of combined therapeutic strategies, suggesting PDI may be particularly useful in situations where heterogeneity within resistant bacterial populations limits the effectiveness of antibiotics. The results reinforce the hypothesis that PDI not only increases the susceptibility of bacterial strains to antibiotics^{16,17,27,50,51}, but also promotes a more homogeneous bacterial population in terms of antimicrobial susceptibility. That homogenization may be a critical factor in the successful treatment of resistant bacterial infections, paving the way for the use of PDI as a valuable adjuvant in antimicrobial therapy.

Antimicrobial resistance is a complex topic since it involves various responses by the microorganism to the antimicrobial agent, from changes in genetic expression to phenotypic adaptations. As a result, heterogeneity within populations interferes with the response to antibiotics, and resistant or persistent subpopulations are common. Therefore, understanding the sensitivity profile of bacterial strains should go beyond MIC analyses and include population analyses so that treatments for combating antimicrobial resistance would take into account the multiple layers of the scenario. In such a case, the results show the increase in susceptibility after treatment with PDI reduces the MIC of antibiotics of different classes and the photodynamic action impacts the subpopulations, leaving bacterial cells with a more homogeneous profile in response to antibiotic therapy and increasing the chances of successful treatments in infection control.

Methodology

Cultivation of microorganisms

Staphylococcus aureus clinically isolated and with ATCC25923 reference were cultivated in Brain Heart Infusion (BHI) Agar for 24 h at 37 °C for their optimal growth. After incubation, selected colonies were carefully suspended in phosphate-buffered saline (PBS) for photodynamic inactivation (PDI) tests. Mueller Hinton (MH) medium, recognized for its ability to sustain the phenotypic expression of resistance, was used for trials involving antimicrobial treatments. The inoculum was standardized to a bacterial density of 10⁸ Colony Forming Units per milliliter (CFU/ml) by the calibration of absorbance at 600 nm by a Varian's Cary UV-Vis50 spectrophotometer. Such a density was chosen because it reflects a significant bacterial load ideal for evaluations of the effectiveness of PDI and antimicrobial treatments under standardized conditions.

Antibiotic-induced *Staphylococcus aureus* strains: *S. aureus* bacteria (ATCC25923) were subjected to culture cycles in MH medium containing 1/4 of the MIC of the corresponding antibiotic. They were kept in contact for 24 h, washed at 3000 rpm and resuspended in MH for 10⁸ CFU/ml standardization. Contact was maintained for 72 h and the new MIC of the cultured colonies was checked^{30,52}.

Photodynamic inactivation

The stock solution of synthetic PS curcumin (EMIPharma) was prepared in 5 mM ethyl alcohol and diluted in distilled water at the concentrations of interest. The concentration of ethyl alcohol was substantially reduced to avoid possible adverse effects, with a 0.2% final one. Three control groups, namely General Control (bacteria), Dark Control (bacteria + PS), and Light Control (bacteria + light), and one treatment group PDI (bacteria + PS + light) were employed. For PDI and dark groups, the bacteria were incubated with 10 µM of CUR for 15 min. Subsequently, the light and PDI groups were subjected to a light dose in the 10 J/cm² range by a 450 nm LED lighting device (Biotable). The samples were seeded in Petri dishes for the counting of the surviving colony-forming units per milliliter (CFU/ml). Equation 1, where “D” is the light dose, “I” is the intensity of the irradiation device, and “t” is the irradiation time, calculated the light dose:

$$D = I \cdot t \quad (1)$$

Conditions below the PDI dose limit were used for the combined experiments, ensuring the survival of the bacterial cells throughout the 5 treatment cycles. At each cycle, the bacterial sample was separated into two groups - one to check the MIC of the antibiotics and another to be cultivated in a BHI culture medium for 6 h before a subsequent PDI treatment. The protocol followed the sequence of initial incubation, exposure to light (10 J/cm²), and sample collection at 6-hour intervals, for all stages of the 5 treatment cycles. After each PDI cycle,

cell viability was checked to confirm the survival of the bacterial cells and ensure that the conditions were within the PDI treatment limit³⁰.

Minimum inhibitory concentration

The experiments followed the recommendations of the Brazilian Committee for Antimicrobial Sensitivity Testing - BrCAST⁴⁴. Antimicrobials amoxicillin (AMO), erythromycin (ERY), and gentamicin (GEN) were distributed in 96-well plates by sequential dilution. The MIC study was carried out with an initial concentration of 10⁶ CFU/ml of bacterial cells added to each well of the 96-well plate. A positive control of bacterial growth and a negative control of the culture medium were conducted together and the plate was stored at 37 °C for 24 h. 30 µL of resazurin solution (0.015%) were added for 4 h at 37 °C. The minimum inhibitory concentration (MIC) was defined as the lowest concentration of the antibiotic capable of inhibiting the visible growth of the bacterial strains by converting resazurin into resorufin. The classic MIC values for the *S. aureus* strains tested have been included as a reference: for amoxicillin, the MIC ranges from 0.25 to 2 µg/mL in sensitive strains and may exceed 8 µg/mL in resistant strains; for erythromycin, the MIC is 0.25 to 1 µg/mL in susceptible strains and greater than 8 µg/mL in resistant strains; and for gentamicin, the MIC is ≤ 1 µg/mL in susceptible strains and ≥ 16 µg/mL in resistant strains.

Analysis of the distribution of population mortality curves

The PDI cycles were applied exposing the bacterial culture at different intervals. Before and after the cycles, MIC was determined and the optical density at 600 nm was collected with the use of a plate reader (Multiskan™ Fc Microplate Photometer). The mortality fraction was recorded as a function of the different concentrations of antibiotics evaluated³⁰ and later normalized from 0 to 1. Functions that best described the behavior of population mortality were explored for mathematical analyses of the data. Equations 2 and 3 indicated that two logistic functions were the most suitable for fitting the experimental data, yielding the lowest χ^2 value. From the mortality curve, the plotted derivative provided parameters of the population distribution through full width at half height (FWHM) analysis^{46,47,53}.

$$y = \frac{a}{1 + b \cdot \exp(-k \cdot x)} \quad (2)$$

$$y = \frac{a}{1 + \exp(-k \cdot (x - x_c))} \quad (3)$$

The parameter a represents the maximum mortality achievable by the antibiotic, b and k indicates the rate of change in mortality, and x_c represents the point at which the response to the antibiotic begins to be more pronounced (i.e., the minimum dose required to observe a significant effect).

Data availability

The datasets used and/or analysed during the current study available from the corresponding author on reasonable request.

Received: 16 July 2024; Accepted: 12 November 2024

Published online: 16 November 2024

References

- Hanage, W. P. Not so simple after all: Bacteria, their population genetics, and recombination. *Cold Spring Harb Perspect. Biol.* **8**, (2016).
- Grote, J., Krysiak, D. & Streit, W. R. Phenotypic Heterogeneity, a Phenomenon That May Explain Why Quorum Sensing Does Not Always Result in Truly Homogenous Cell Behavior. *Appl Environ Microbiol* **81**, 5280–5289 (2015).
- Band, V. I., Weiss, D. S. & Heteroresistance A cause of unexplained antibiotic treatment failure? *PLoS Pathog.* **15**, e1007726 (2019).
- Aslam, B. et al. Antibiotic resistance: a rundown of a global crisis. *Infect. Drug Resist.* **11**, 1645–1658 (2018).
- Sommer, M. O. A., Munck, C., Toft-Kehler, R. V. & Andersson D. I. Prediction of antibiotic resistance: time for a new preclinical paradigm? *Nat. Rev. Microbiol.* **15**, 689–696 (2017).
- Adediji, W. A. The treasure called antibiotics. *Ann. Ib. Postgrad. Med.* **14**, 56–57 (2016).
- Tacconelli, E. et al. Discovery, research, and development of new antibiotics: the WHO priority list of antibiotic-resistant bacteria and tuberculosis. *Lancet Infect. Dis.* **18**, 318–327 (2018).
- WHO. Global priority list of antibiotic-resistant bacteria to guide research, discovery, and development of new antibiotics. *Who* **7** (2017).
- O'Neill, J. Tackling drug-resistant infections globally: fi Nal report and recommendations. The review on antimicrobial resistance. *Rev. Antimicrob. Resist.* (2016).
- Pulingam, T. et al. Antimicrobial resistance: prevalence, economic burden, mechanisms of resistance and strategies to overcome. *Eur. J. Pharm. Sci.* **170**, 106103 (2022).
- Cabral, D. J., Wurster, J. I. & Belenky, P. Antibiotic persistence as a metabolic adaptation: Stress, metabolism, the host, and new directions. *Pharmaceuticals* **11**, (2018).
- Ragheb, M. N. et al. Inhibiting the evolution of Antibiotic Resistance. *Mol. Cell.* **73**, 157–165e5 (2019).
- Keren, I., Kaldalu, N., Spoering, A., Wang, Y. & Lewis, K. Persister cells and tolerance to antimicrobials. *FEMS Microbiol. Lett.* **230**, 13–18 (2004).
- Fisher, R. A., Gollan, B. & Helaine, S. Persistent bacterial infections and persister cells. *Nat. Rev. Microbiol.* **15**, 453–464 (2017).
- Band, V. I. et al. Antibiotic combinations that exploit heteroresistance to multiple drugs effectively control infection. *Nat. Microbiol.* **4**, 1627–1635 (2019).
- Soares, J. M., Guimarães, F. E. G., Yakovlev, V. V., Bagnato, V. S. & Blanco, K. C. Physicochemical mechanisms of bacterial response in the photodynamic potentiation of antibiotic effects. *Sci. Rep.* **12**, 21146 (2022).

17. Willis, J. A. et al. Breaking down antibiotic resistance in methicillin-resistant *Staphylococcus aureus*: combining antimicrobial photodynamic and antibiotic treatments. *Proc. Natl. Acad. Sci. U S A* **119**, (2022).
18. Feng, Y., Tonon, C. C. & Hasan, T. Dramatic destruction of methicillin-resistant *Staphylococcus aureus* infections with a simple combination of Amoxicillin and light-activated methylene blue. *J. Photochem. Photobiol. B* **235**, (2022).
19. Barra, F. et al. Photodynamic and antibiotic therapy in combination to Fight biofilms and resistant surface bacterial infections. *Int. J. Mol. Sci.* **16**, 20417 (2015).
20. Jeong, S., Lee, J., Im, B. N., Park, H. & Na, K. Combined photodynamic and antibiotic therapy for skin disorder via lipase-sensitive liposomes with enhanced antimicrobial performance. *Biomaterials*. **141**, 243–250 (2017).
21. Choi, S. S., Lee, H. K. & Chae, H. S. Synergistic in vitro photodynamic antimicrobial activity of methylene blue and chitosan against *Helicobacter pylori* 26695. *Photodiagnosis Photodyn Ther.* **11**, 526–532 (2014).
22. Feng, Y., Tonon, C., Ashraf, C., Hasan, T. & S. Photodynamic and antibiotic therapy in combination against bacterial infections: efficacy, determinants, mechanisms, and future perspectives. *Adv. Drug Deliv. Rev.* **177**, 113941 (2021).
23. Cieplik, F. et al. Antimicrobial photodynamic therapy – what we know and what we don't. *Crit. Rev. Microbiol.* **44**, 571–589 (2018).
24. Liu, Y., Qin, R., Zaat, S. A. J., Breukink, E. & Heger, M. Antibacterial photodynamic therapy: overview of a promising approach to fight antibiotic-resistant bacterial infections. *J. Clin. Transl. Res.* **1**, 140–167 (2015).
25. Hamblin, M. R. & Hasan, T. Photodynamic therapy: a new antimicrobial approach to infectious disease? *Photochem. Photobiol. Sci.* **3**, 436–450 (2004).
26. Bacellar, I., Tsubone, T., Pavani, C. & Baptista, M. Photodynamic efficiency: from Molecular Photochemistry to Cell Death. *Int. J. Mol. Sci.* **16**, 20523–20559 (2015).
27. Willis, J. A. et al. Photodynamic viral inactivation: recent advances and potential applications. *Appl. Phys. Rev.* **8**, 021315 (2021).
28. Awad, M. M., Tovmasyan, A., Craik, J. D. & Batinic-Haberle, I. Benov, L. T. Important cellular targets for antimicrobial photodynamic therapy. *Appl. Microbiol. Biotechnol.* **100**, 7679–7688 (2016).
29. Wainwright, M. et al. Photoantimicrobials—are we afraid of the light? *Lancet Infect. Dis.* **17**, e49–e55 (2017).
30. Soares, J. M., Yakovlev, V. V., Blanco, K. C. & Bagnato, V. S. Recovering the susceptibility of antibiotic-resistant bacteria using photooxidative damage. *Proc. Natl. Acad. Sci. U S A* **120**, (2023).
31. Wiuff, C. et al. Phenotypic tolerance: antibiotic enrichment of noninherited resistance in bacterial populations. *Antimicrob. Agents Chemother.* **49**, 1483–1494 (2005).
32. Blair, J. M. A., Webber, M. A., Baylay, A. J., Ogbolu, D. O. & Piddock, L. J. V. Molecular mechanisms of antibiotic resistance. *Nat. Rev. Microbiol.* **13**, 42–51 (2015).
33. Peterson, E. & Kaur, P. Antibiotic resistance mechanisms in bacteria: relationships between resistance determinants of antibiotic producers, environmental bacteria, and clinical pathogens. *Front. Microbiol.* **9**, 1–21 (2018).
34. Andersson, D. I., Nicoloff, H. & Hjort, K. Mechanisms and clinical relevance of bacterial heteroresistance. *Nat. Rev. Microbiol.* **17**, 479–496 (2019).
35. Liu, Y., Li, R., Xiao, X. & Wang, Z. Bacterial metabolism-inspired molecules to modulate antibiotic efficacy. *J. Antimicrob. Chemother.* **74**, 3409–3417 (2019).
36. Stokes, J. M., Lopatkin, A. J., Lobritz, M. A. & Collins, J. J. Bacterial metabolism and antibiotic efficacy. *Cell. Metab.* **30**, 251–259 (2019).
37. Corona, F. & Martinez, J. L. Phenotypic resistance to antibiotics. *Antibiot.* **2013**, 2, 237–255 (2013).
38. Pourhajibagher, M., Chiniforush, N., Shahabi, S., Ghorbanzadeh, R. & Bahador, A. Sub-lethal doses of photodynamic therapy affect biofilm formation ability and metabolic activity of *Enterococcus faecalis*. *Photodiagnosis Photodyn Ther.* **15**, 159–166 (2016).
39. de Vale, G. H. R. et al. Interplay between ESKAPE pathogens and Immunity in skin infections: an overview of the Major determinants of Virulence and Antibiotic Resistance. *Pathogens*. **10**, 148 (2021).
40. Wozniak, A. & Grinholc, M. Combined antimicrobial activity of photodynamic inactivation and antimicrobials—state of the art. *Front. Microbiol.* **9**, 930 (2018).
41. Wiegand, I., Hilpert, K. & Hancock, R. E. W. Agar and broth dilution methods to determine the minimal inhibitory concentration (MIC) of antimicrobial substances. *Nat. Protoc.* **3**, 163–175 (2008).
42. Ezadi, F., Ardebili, A. & Mirnejad, R. Antimicrobial susceptibility testing for polymyxins: challenges, issues, and recommendations. *J. Clin. Microbiol.* **57**, 10–1128 (2019).
43. González-Cabaleiro, R., Mitchell, A. M., Smith, W., Wipat, A. & Ofiteru, I. D. Heterogeneity in pure microbial systems: experimental measurements and modeling. *Front. Microbiol.* **8**, 1813 (2017).
44. BRCast. Brazilian Committee on Antimicrobial Susceptibility Testing. (2023).
45. Kowalska-Krochmal, B. & Dudek-Wicher, R. The minimum inhibitory concentration of antibiotics: methods, interpretation, clinical relevance. *Pathogens* **10**, 165 (2021).
46. Soares, J. M., Inada, N. M., Bagnato, V. S. & Blanco, K. C. Evolution of surviving *Streptococcus pyogenes* from pharyngotonsillitis patients submit to multiple cycles of antimicrobial photodynamic therapy. *J. Photochem. Photobiol. B*. **210**, 111985 (2020).
47. Sabino, L. G. et al. Experimental evidence and model explanation for cell population characteristics modification when applying sequential photodynamic therapy. *Laser Phys. Lett.* **8**, 239–246 (2011).
48. Abd El-Aleam, R. H., George, R. F., Georgey, H. H. & Abdel-Rahman, H. M. Bacterial virulence factors: a target for heterocyclic compounds to combat bacterial resistance. *RSC Adv.* **11**, 36459–36482 (2021).
49. Vatansever, F. et al. Antimicrobial strategies centered around reactive oxygen species – bactericidal antibiotics, photodynamic therapy, and beyond. *FEMS Microbiol. Rev.* **37**, 955–989 (2013).
50. Aroso, R. T. et al. Synergic dual phototherapy: Cationic imidazolyl photosensitizers and ciprofloxacin for eradication of in vitro and in vivo *E. coli* infections. *J. Photochem. Photobiol. B*. **233**, 112499 (2022).
51. Dastgheyb, S. S., Eckmann, D. M., Composto, R. J. & Hickok, N. J. Photo-activated porphyrin in combination with antibiotics: therapies against *Staphylococci*. *J. Photochem. Photobiol. B*. **129**, 27–35 (2013).
52. Van Den Bergh, B. et al. Frequency of antibiotic application drives rapid evolutionary adaptation of *Escherichia coli* persistence. *Nat. Microbiol.* **1**, 1–7 (2016).
53. de Faria, C. M. G., Inada, N. M., Vollet-Filho, J. D. & Bagnato, V. S. A threshold dose distribution approach for the study of PDT resistance development: a threshold distribution approach for the study of PDT resistance. *J. Photochem. Photobiol. B*. **182**, 85–91 (2018). Heterogeneity in Figure 1 is misspelled (it says “heterogeneity”)

Acknowledgements

This research was financially supported by FAPESP (2013/07276-1, 2014/50857-8, and 2024/00100-0), CNPq (465360/2014-9 and 384511/2023-6), CPRIT (M20301556), GURI (M230930) and CRI (02-292034). Also, the Air Force Office of Scientific Research (FA9550-20-1-0367, FA9550-23-1-0599), the National Institutes of Health (NIH) (R01GM152633 and 1R21CA269099).

Author contributions

Conceptualization: J.M.S., V.S.B., K.C.B.; V.V.Y.; Methodology: J.M.S., V.S.B., K.C.B.; Investigation: J.M.S.; Supervision: V.S.B., K.C.B.; Writing—original draft: J.M.S.; Writing—review editing: J.M.S., V.V.Y., K.C.B., V.S.B.

Declarations

Competing interests

The authors declare no competing interests.

Additional information

Correspondence and requests for materials should be addressed to J.M.S.

Reprints and permissions information is available at www.nature.com/reprints.

Publisher's note Springer Nature remains neutral with regard to jurisdictional claims in published maps and institutional affiliations.

Open Access This article is licensed under a Creative Commons Attribution-NonCommercial-NoDerivatives 4.0 International License, which permits any non-commercial use, sharing, distribution and reproduction in any medium or format, as long as you give appropriate credit to the original author(s) and the source, provide a link to the Creative Commons licence, and indicate if you modified the licensed material. You do not have permission under this licence to share adapted material derived from this article or parts of it. The images or other third party material in this article are included in the article's Creative Commons licence, unless indicated otherwise in a credit line to the material. If material is not included in the article's Creative Commons licence and your intended use is not permitted by statutory regulation or exceeds the permitted use, you will need to obtain permission directly from the copyright holder. To view a copy of this licence, visit <http://creativecommons.org/licenses/by-nc-nd/4.0/>.

© The Author(s) 2024